

STUDY OF A FAR INFRARED CAVITY AT 60 μm AND 100 μm IRAS MAP AROUND THE CARBON-RICH AGB STAR AT GALACTIC LATITUDE 8.6 $^\circ$

A.K. Gautam and B. Aryal

Central Department of Physics, T.U., Kirtipur, Kathmandu, Nepal.

Abstract: In this paper, we discussed about the dusty environment of the far infrared cavity around the AGB star located at R.A. (J2000) = 01^h41^m 01^s and Dec (J2000) = 71 $^\circ$ 04' 00", lying within far infrared loop G125+09⁶ in the far infrared IRAS maps. A cavity like structure (major diameter $\sim 2.55\text{pc}$ & minor diameter $\sim 0.77\text{pc}$) is found to lie at R.A. (J2000) = 01^h46^m57.2^s and DEC (J2000) = 71 $^\circ$ 24'57.1", located at a distance $\sim 220\text{pc}$ from the star. We studied the distribution of flux density, dust color temperature, dust mass, visual extinction in the cavity. We further studied the distribution Planck function along extension and compression, distribution of dust color temperature along square of the major and minor diameters. The dust color temperature is found to lie in the range (19.7 \pm 1.25) K to (21.1 \pm 0.55)K which shows the cavity is isolated and stable. A possible explanation of the results will be discussed.

Keywords: Far infrared cavity; AGB stars; Dust color temperature; Dust mass.

INTRODUCTION

There are three types of stars according to their mass. They are low mass stars, intermediate mass stars and massive stars. Their proportion in existence is 1: 10: 1000. Most of the stars spend their half life in main sequence. When fusion of hydrogen is exhausted in the main sequence, the star leaves the main sequence and rises up towards right side. This stage of evolution is called red giant branch (RGB) phase. During this phase, the star expands but core contracts as a result luminosity increases. As the luminosity reaches nearly $10^3 L_\odot$, inert He core burns means He shell flash takes place and the star moves horizontally with almost constant luminosity. This stage of stellar evolution is called horizontal branch (HB). After around 10^8 years, He core exhausts. At this condition, He core leaves its space and two burning shells i.e. H-burning shell and He-burning shell are produced leaving C/O core as a result the star moves up parallel to RGB which is called asymptotic giant branch (AGB).

For low mass stars having masses $< 0.8M_\odot$, there is not sufficient temperature for fusion of hydrogen so that they can't change in to Asymptotic giant branch (AGB) stars. Actually low and intermediate mass stars in the range ($0.8M_\odot < M < 8.0M_\odot$) are the AGB stars which is the final nuclear burning stage. This phase of evolution is characterized by two nuclear burning shell of hydrogen and helium where hydrogen burning shell lies below the convective envelope and helium burning shell lies above the electron-degenerate core of carbon and oxygen, or for the most massive AGB stars a core of oxygen, neon, and magnesium.³ This AGB stage is characterized by low surface effective temperatures (below 3500K) and intense mass loss (from 10^{-7} to $10^{-4}M_\odot\text{yr}^{-1}$)⁸.

Interstellar medium consists matter and field. Matter contains gas and dust. First evidence of dust in the ISM was first justified by interstellar extinction curve. Dusty

circumstellar envelopes will format the distance of several stellar radii. Dust grains in the envelopes absorb stellar radiation say uv radiation and re-emist infrared radiation so AGB stars are important infrared sources. The mass loss process plays an important role in the evolution of AGB stars. Statistics of a large sample of AGB stars would help to constrain the evolution of dust envelope. There are mainly three types of AGB stars: the O-rich with $C/O < 1$ and mainly silicate-type grains in the outflow, C-rich with $C/O > 1$ and mainly carbonaceous grains in the envelopes and S-type with $C/O \sim 1$. Due to different dust compositions of these AGB stars, different infrared spectral features are obtained which can be used to distinguish the groups of the stellar objects .

He-core burning phase is about 10 times shorter than the H-core burning shell so that the He-core burning leaves a C/O core behind that is surrounded by both a hydrogen and helium burning shell. For low and intermediate mass stars, carbon doesn't ignite and C/O core contracts and becomes electron degenerate. During the early AGB phase, the abundance of He in the centre goes to zero where He-burning continues in a shell around a degenerate C-O core. In the meantime, the H- layer around the helium shell expands and cools sufficiently so that hydrogen burning shell is extinguished. Convective envelope sets in and moves inwards and second dredge-up takes place. He shell is the main source for nuclear production so that it burns outward and reaches the hydrogen shell. In case of thermally pulsating AGB phase, helium shell becomes thin and remains thermally unstable as a result thermal pulses are produced. In each thermal pulse, luminosity of helium shell nearly approaches $10^8 L_\odot$ ⁵. The production of such high luminosity in helium shell is called He shell flash or thermal pulse which is used to expand the outer layers. Such strong expansion drives the H shell cooler and less dense as a result H shell is extinguished. The inner edge

Author for Correspondence : A.K. Gautam, Central Department of Physics, T.U., Kirtipur, Kathmandu, Nepal.
Email: arjungautamnpj@gmail.com

of deep convective envelope can then move inward and mix to the surface products of internal nucleosynthesis. This mixing process which occurs periodically after each TP is known as third dredge-up which is the mechanism for producing carbon stars. During TP-AGB phase, main dominant source of nuclear energy is the hydrogen shell. Thermally pulsating AGB phase is the phase after the first thermal pulse to the time when the star ejects its envelope.

METHODS

We investigated a cavity-like structure in both 60 and 100 micron IRAS maps around a AGB star. We briefly

In this paper, we study the physical properties of far infrared cavity, that we investigated during a systematic search on IRAS maps, located close to a carbon-rich AGB star named AGB01+71 at 8.6°Galactic latitude. In section 2, we describe methods of calculation. A brief description of the result and discussion will be given in the section 3. Finally, we conclude our results in the section 4.

describe a method for calculation of dust color temperature, dust mass and visual extinction of the dusty environment around carbon-rich Asymptotic Giant Branch named AGB01+71.

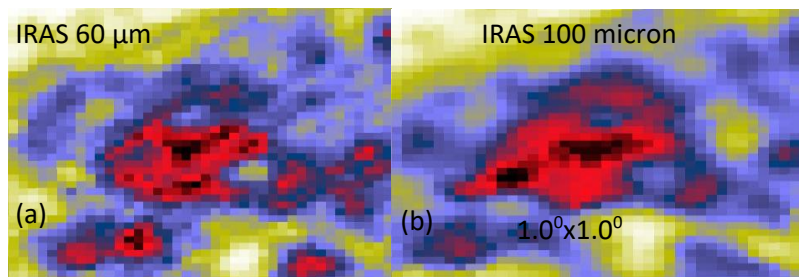


Figure: 1. (a) and (b) are the JPEG images of the far infrared cavity at 60 μm and 100 μm IRAS maps around the AGB 01+71 centered at R.A. (J2000) = 01^h46^m57.2^s, Dec. (J2000) = 71°24' 57.1", located within far infrared loop G125+09.

2.1 Dust Color Temperature

For the calculation of dust color temperature, we adopt the method proposed by Schnee et al.⁷ and Dupac et al.². According to Schnee et al.⁷, dust color temperature of the emission at a wavelength λ_i is given by,

$$T_d = \frac{-96}{\ln\{R \times 0.6^{(3+\beta)}\}} \dots \dots \dots (1)$$

where, $R = \frac{F(60 \mu m)}{F(100 \mu m)}$

$F(60 \mu m)$ and $F(100 \mu m)$ are the flux densities in 60 μm and 100 μm respectively and Eq. (1) is used for calculation of the dust color temperature. The spectral emissivity index (β) depends on dust grain properties like composition, size, and compactness. For a pure blackbody would have $\beta = 0$, the amorphous layer-lattice matter has $\beta \sim 1$, and the metals and crystalline dielectrics have $\beta \sim 2$ which is used in our calculations.

2.2 Planck's Function

The value of Planck's function depends on the wavelength (frequency), and hence the temperature. Finally it is used to calculate dust mass. In 1900, Planck proposed a relation which is named as Planck's function. According to him, the Planck's function is given by

$$B(\nu, T) = \frac{2h\nu^3}{c^2} \left[\frac{1}{e^{\left(\frac{h\nu}{kT}\right)} - 1} \right] \dots \dots \dots (2)$$

where, h = Planck's constant, c = velocity of light, ν = frequency at which the emission is observed,

λ = wavelength of the radiation and T = temperature of each pixel.

2.3 Dust Mass

For the calculation of dust mass, first we need the value of flux density (F_ν) at 100 μm maps and we use the expression given by⁴,

$$M_d = \frac{4a\rho}{3Q(\nu)} \frac{F(\nu)D^2}{B(\nu, T)} \dots \dots \dots (3)$$

where, weighted grain size (a) = 0.1 μm, grain density (ρ) = 3000 kg m⁻³, grain emissivity (Q_ν) = 0.0010 (for 100 μm)¹⁰. So the equation (3) reduces to,

$$M_{dust} = 0.4 \left[\frac{S_\nu D^2}{B(\nu, T)} \right] \dots \dots \dots (4)$$

We use equation (4) to calculate dust mass of the cavity.

RESULT AND DISCUSSION

3.1 Structure: Contour Maps

During the systematic search on IRAS maps, we found an isolated far infrared cavity in the 100 μm and 60 μm IRAS maps at R.A. (J2000) = 01^h 46^m 57.2^s, Dec. (J2000) = 71° 24' 57.1", located within far infrared loop G125+09. With the help of the software ALADIN2.5, we have studied size, dust color temperature, dust mass, inclination angle and visual extinction of the cavity. We selected contour level 1-85 in such a way that it circles the cavity. JPEG images of the cavity at 60 μm and 100 μm IRAS map are shown in the fig.1 (a) and (b) respectively.

3.2 Distribution of Flux Density

Using ALADIN2.5 software, flux densities at 60 μ m and 100 μ m have measured. The flux density distribution within the contour of the region of interest has studied. We have plotted a graph between (100) and F(60) with the help of ORIGIN 5.0 which is shown in fig.2(a). From

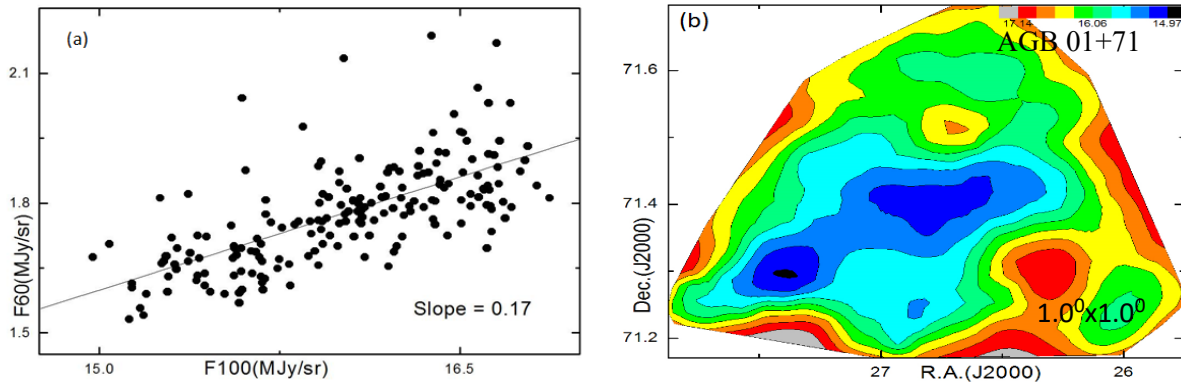


Figure: 2(a) The 100 μ m versus 60 μ m flux density in the region of interest and 2(b) Contour map at 100 μ m flux density where the AGB star is located at the center R.A. = 01^h 46^m 57.2^s, Dec. (J2000) = 71^o 24' 57.1".

Again distribution of flux density at 100 μ m of the pixels within the contour level with right ascension (R.A.) and declination (Dec.) are plotted in contour map by using ORIGIN 8.0 and is shown in fig.2(b). Graph shows that all the fluxes from minimum to maximum lie within the contour level. Most of the maximum flux regions lie at the boundary.

3.3. Dust color Temperature and its Variation

Using the method of Schnee et al.⁷, we calculated dust color temperature of each pixel inner the outer isocontour

the linear fit, slope of the line was 0.17, correlation coefficient (R)= 0.68. The linear equation of the fitted line is, $y = -1.01 + 0.17x$. Using the slope of best fitted plot, dust color temperature is found as 22.2 K which is used to calculate error in calculated dust color temperature.

in the region of interest. We use the IRAS 100 μ m and 60 μ m FITS images downloaded from the IRAS server. For the calculation of temperature we choose the value of $\beta = 2$ following the explanation given by². Variation of temperature with corresponding R.A.(J2000) and Dec.(J2000) are plotted by using ORIGIN 8.0 and the graph is shown in figure 3(a). Graph shows that temperature distributions are in separate cluster but minimum temperature region is little bit shifted from minimum flux density which is unusual behaviour. Such type of nature is obtained due to external factors.

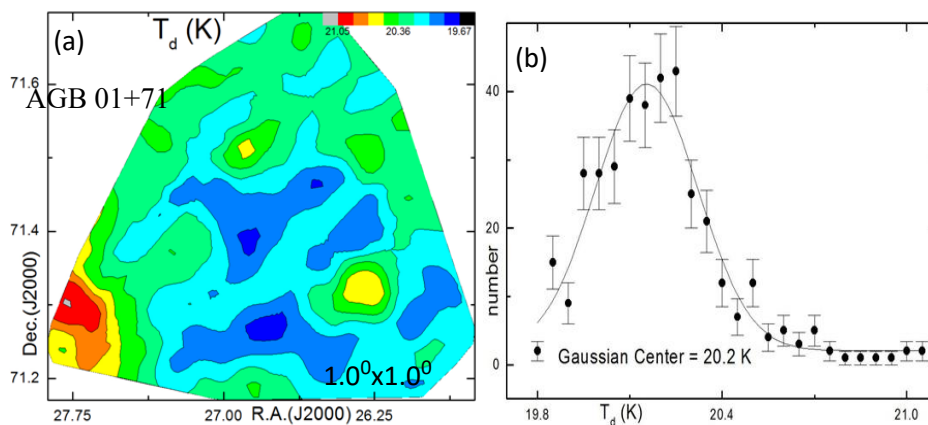


Figure: 3 (a) Contour map of dust color temperature and (b) Gaussian fit of dust color temperature. The far infrared cavity is centered at R.A. = 01^h 46^m 57.2^s, Dec. (J2000) = 71^o 24' 57.1".

The region in which minimum and maximum temperature is found in the range (19.7 \pm 1.25) K to (21.1 \pm 0.55) K with low offset temperature. Such low offset temperature variation shows that there is symmetric outflow or symmetric distribution of density and temperature. It further suggests that particles are independently vibrating. Gaussian fit of dust color temperature is more or less

following the Gaussian distribution with positive skewness. When this result is compared with the result obtained in¹ where temperature variation is 20K to 22K so our result is also comparable with that result. In the contour map, minimum flux and minimum temperature region are shifted which is due to some external factors possibly due to AGB wind.

3.4. Size of the Structure

Major and minor diameter of the structure can be easily calculated by using a simple expression i.e., $L = R \times \theta$, where $R = 220\text{pc}$ is the distance of the structure and $\theta =$ pixel size (in radian). After calculation the major and minor diameter of the cavity are found to be 2.55 pc and 0.77 pc respectively. Thus, the size of the structure is $2.55\text{ pc} \times 0.77\text{ pc}$.

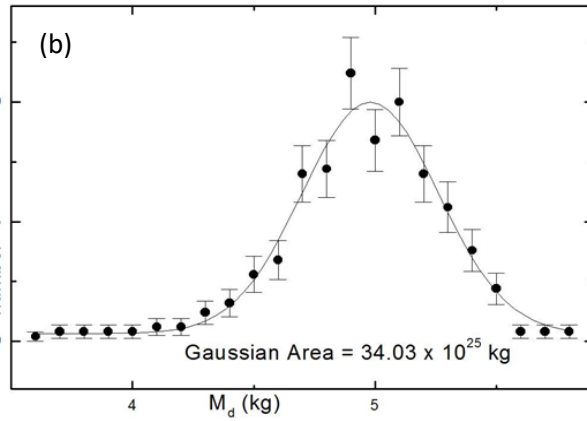
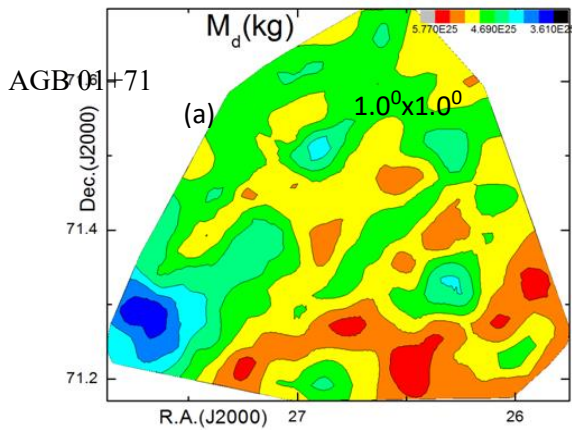


Figure: 4(a) contour map of dust mass and (b) Gaussian fit of dust mass. The far infrared cavity is centered at R.A. = $01^{\text{h}} 46^{\text{m}} 57.2^{\text{s}}$, Dec. (J2000) = $71^{\circ} 24' 57.1''$.

Distribution of dust mass in the contour map is shown in figure 4(a) which shows that minimum temperature region is denser and lie at the maximum mass region in the selected contour which is usual trend and. It means distribution of dust mass follow cosmological principle i.e their distribution is homogeneous and isotropy. Figure 4(b) is the Gaussian fit where the data more or less follow Gaussian distribution with negative skewness.

3.6 Distribution of Planck Function with Diameters

Figure 5(a) and (b) show the distribution of Planck function along extension and compression where the data

3.5. Dust Mass Estimation and its Variation

For the calculation of dust mass, we need the distance to the region of interest. The distance of the structure is 220pc . By using the temperature of each pixel and corresponding distance of the structure, we calculated mass of each pixel. Average mass of each pixel is $4.91 \times 10^{25}\text{kg}$ and total mass of the structure is $1.86 \times 10^{28}\text{ kg}$ i.e $0.0094M_{\odot}$. But mass of dust obtained around white dwarf WD 1003-44 in¹ is $0.08M_{\odot}$. It means mass of dust around AGB Star is less than White Dwarf.

are distributed randomly with very low correlation coefficient ($R = -0.03$ in case of minor diameter but in case of major diameter, $R = -0.43$). There is no systematic trend of their distribution in both cases. It means distribution is non uniform and is not following the Maxwell velocity distribution which is possibly due to near by AGB wind. Same nature and result is obtained in the linear fit of the scattered plot between dust color temperature and square of the major and minor diameter which is shown in figure 6(a) and (b).

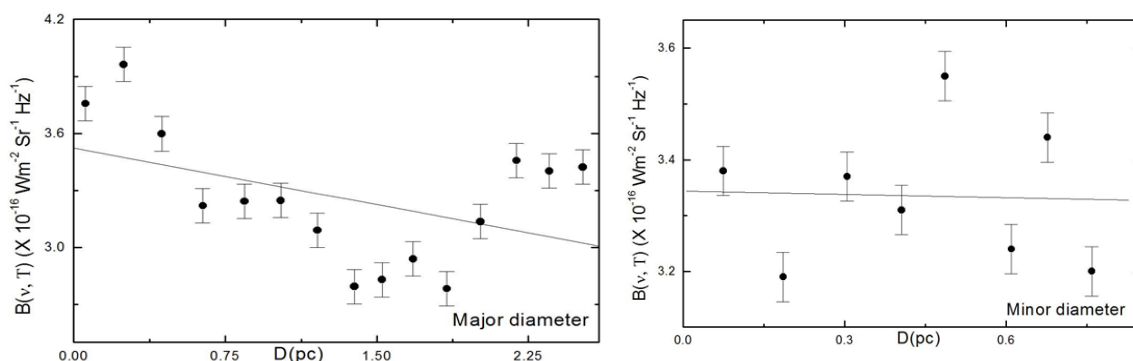


Figure: (5)(a) Linear fit of scattered plot between major diameter and Planck function and (b) Linear fit of scattered plot between minor diameter and Planck function of the cavity centered at R.A. = $01^{\text{h}} 46^{\text{m}} 57.2^{\text{s}}$, Dec. (J2000) = $71^{\circ} 24' 57.1''$.

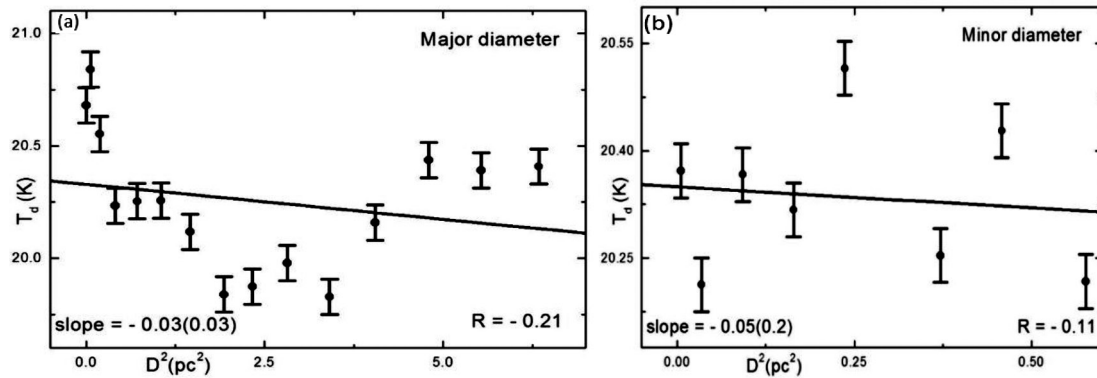


Figure: (6):(a) Linear fit of scattered plot between square of the major diameter and dust color temperature and (b) Linear fit of scattered plot between square of the minor diameter and dust color temperature of the cavity centered at R.A. = $01^{\text{h}} 46^{\text{m}} 57.2^{\text{s}}$, Dec. (J2000) = $71^{\circ} 24' 57.1''$.

3.7. Variation of Visual Extinction with Dust Color Temperature

Figure (7) is a linear fit of the scattered plot between visual extinction and dust color temperature. The graph shows a systematic trend with high correlation coefficient i.e., -0.92 , which shows that there is best correlation between the data. From the linear fit, we found a new relation between visual extinction and dust color temperature. The relation is $\log(A_V \times T_d) = -3.9$. It means $(A_V \times T_d) < 1$ i.e., higher the extinction, lower the dust color temperature and vice versa.

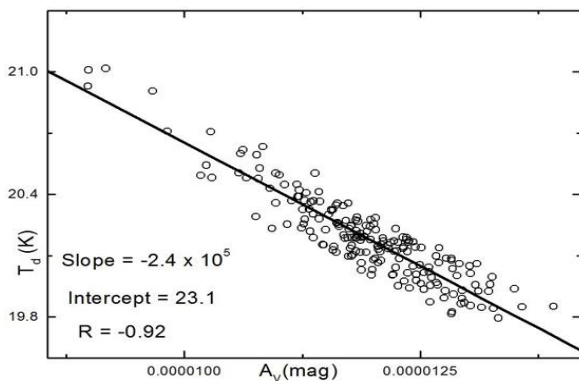


Figure 7: A linear fit of the scattered plot between visual extinction and dust color temperature of the far infrared cavity centered at R.A. = $01^{\text{h}} 46^{\text{m}} 57.2^{\text{s}}$, Dec. (J2000) = $71^{\circ} 24' 57.1''$.

CONCLUSION

The physical properties of the far infrared cavity around the AGB01+71 star located within far infrared loop G125+09 are measured and analyzed. From the calculated value, distribution of flux density, dust color temperature, Planck function, dust mass and visual extinction of the cavity were studied. Following are the conclusions:

- The major and minor diameter of the far infrared cavity was found to be 2.55pc and 0.77 pc respectively.
- The maximum temperature (21.1 ± 0.55) K was found at R.A.(J2000)= 27.82° & Dec.(J2000)= 71.31° and minimum temperature(19.7 ± 1.25) K was found at

R.A.(J2000)= 26.78° & Dec.(J2000)= 71.26° , with low offset temperature which suggests that the cavity is isolated and stable.

- In general, minimum flux and minimum temperature lie at same point in the pixel but in this case minimum temperature is shifted which may be due to external factors, possibly wind emitted from the AGB star. Similarly maximum temperature region is the densest region which is normal behavior. It means distribution of dust mass follow cosmological principle.
- Total mass of the cavity was found to be $1.86 \times 10^{28}\text{kg}$ and that of average mass was $4.91 \times 10^{25}\text{ kg}$.
- Linear fit of scattered plot between visual extinction and dust color temperature shows that there is a systematic trend and visual extinction decreases with increase in dust color temperature and vice-versa.

We intend to study the role of carbon-rich AGB star to form the far-infrared cavity in the future.

ACKNOWLEDGEMENTS

We are grateful to the Department of Astro-Particle Physics, Innsbruck University, specially to Prof. R. Weinberger for invoking us to work on dusty environments around AGB stars. This research has made use of SkyView Virtual Observatory, Aladin v2.5 and NASA/IPAC Extragalactic Database (NED). One of the authors (AKG) acknowledges Central Department of Physics, T.U., Nepal for providing various support of Ph.D.

REFERENCES

1. Aryal, B. & Weinberger, R. 2011. Dust structure around White Dwarf WD 1003-44 in 60 and $100\mu\text{m}$ Iras Survey. *The Himalayan Physics*. **II**: 5-10.
2. Dupac, X., Bernard, J.P., Boudet, N., Giard, M., Lamarre, J.M., Meny, C., Pajot, F., Ristorcelli, I., Serra, G., Stepnik, B. & Torre, J.P. 2003. Inverse Temperature Dependence of the Dust Sub millimeter Spectral Index. *Astronomy & Astrophysics*. **404**: L11-L15.
3. Herwig, F. 2005. Evolution of Asymptotic Giant Branch Stars. *Annu. Rev. Astron. Astrophys.* **43**: 435-479.

4. Hildebrand, R.H. 1983. The determination of cloud mass and dust characteristics from sub millimeter thermal emission. *Royal Astronomical Society*. **24**: 267-282.
5. Karakas, A.I., Lattanzio, J.C. & Pols, O.R. 2002. Parameterising the third dredge-up in asymptotic giant branch stars. *Astron. Soc. Aust.* **19**: 515-38.
6. Konyves, V., Kiss, Cs., Moor, A., Kiss, Z.T., & Toth, L.V. 2007. Catalog of Far- Infrared Loops in the Galaxy. *Astronomy & Astrophysics*. **463**: 1227-1234.
7. Schnee, S.L., Ridge, N.A., Goodman, A.A. & Jason, G.L. 2005. A Complete Look at the Use of IRAS Emission Maps to Estimate Extinction and Dust Temperature. *The Astrophysical Journal*. **634**: 442-450.
8. Seiss, L. & Pumo, M.L. 2006. Evolutionary Properties of Massive AGB Stars. *Memorie della Societa Astronomica Italiana*. **77**: 822-827..
9. Suh, K.W. & Kwon, Y.J. 2009. A Catalog of AGB Stars in IRAS PSC. *Journal of the Korean Astronomical Society*. **42**: 81-91.
10. Young, K., Phillips, T.G. & Knapp, G.R. 1993. Circumstellar Shells Resolved in IRAS Survey Data II. Analysis. *Astrophysical Journal*. **409**: 725-738.

